DOI: 10.51153/kjcis.v7i2.225

Rice Varieties (LULC) Classification using Artificial Neural Network through Landsat 8 OLI Image

Talha Virk [1], Muhammad Usman [2]

1Khwaja Fareed University of Engineering and Information Technology, Rahim Yar Khan, Pakistan, 64200
2Khwaja Fareed University of Engineering and Information Technology, Rahim Yar Khan, Pakistan, 64200

Corresponding Author: *Muhammad Usman (musmanryk@gmail.com)*

Abstract

Multi-temporal and multi-spectral remote sensing images are good instruments that may help traditional agricultural systems by properly monitoring and calculating crop yields prior to harvesting. Traditional agricultural systems mostly depend on limited ground-survey data. Time-series satellite images of vegetation phenology serve a significant role in vegetation monitoring and land-cover categorization because they can record vegetation information at various development phases. It's impossible to overstate how important remote sensing has become in the last several decades. In order to monitor land surface dynamics, natural resource management, and the general status of the ecosystem, remote sensing sensors have been used from space. In order to begin vegetation conservation and restoration projects, it is necessary to know the existing status of plant cover. Several early studies of ecosystems and land cover have used agricultural census data to map paddy rice fields at the global and regional scales.

Keywords: Land Use / Land Cover, Crop Classification, Remote Sensing, Machine Learning

1. Introduction

It is necessary and a necessity to have a timely and accurate forecast of yield at a broad scale in order to reduce climate risk and assure food security, particularly in light of climate change and the growing frequency of severe weather events. Rice is one of the most significant agricultural goods in the world, and Pakistan has a unique position in this regard due to the country's yearly output of more than 7.2 million metric tons of rice. Wheat is the most important agricultural product in the world. Because there are many diverse circumstances and limits, the evaluation of crop output plays a significant part in the process of formulating agricultural policy. Rice yield estimation is an important component of overall food security. Any shift in the values of the effective parameters has the potential to induce shifts in rice yield, which in turn will have an impact on the population's ability to maintain a stable diet. It’s impossible to overstate how important remote sensing has become in the

last several decades. In order to monitor land surface dynamics, natural resource management, and the general status of the ecosystem, remote sensing sensors have been used from space [1]. Here, plant, soil, and water are the earth's surface elements that are being discussed. The spectral signature of a substance may be used to identify it if the sensing system has enough spectral resolution to differentiate it from other materials' spectral signatures. Based on this presumption, multispectral remote sensing may be carried out. Paddy rice field detection and selection is an essential part of getting more precise information about agricultural water consumption in order to efficiently manage fresh water resources [2].

Previous studies of land cover and ecosystems have used agricultural census data to map paddy rice fields at the regional and global scales. These datasets were created late in the 1980s and in the early 1990s, and they were used to analyze global climate and greenhouse gas emissions. It has recently been common practice to combine agricultural census data up to national level to study paddy rice growing areas [3][4]. Self-sufficiency potential must be established in order to estimate rice output. When it comes to calculating rice output, farmers are often asked to provide information on their crop. An alternative approach is collecting a sample of rice grains and then multiplying that number by the overall harvest area, which gives an estimate of rice output. During harvesting times, both rice production estimate techniques are used. As a result, it is critical to know how rice fields are laid out in order to manage water resources and estimate gas emissions. It is important to know the land cover features of rice plants. During the rice life cycle, rice land coverage fluctuates. During the growing season, water covers almost the whole area of irrigated rice fields. There is a maximum rice vegetation coverage (the age of rice =2 months) and then a progressive decline until the time of its harvest [5]. Using satellite remote sensing technology to monitor land use and changes in land cover has been widely used and well accepted.

Time-series satellite photos of vegetation phenology serve a significant function in tracking vegetation and land-cover categorization because they can record vegetation information at various development phases. It has been widely used in paddy-rice monitoring and mapping during the previous several decades, particularly optical remote-sensing pictures.

Because of their high temporal and moderate geographical resolution, MODIS data have been used to map rice all over the globe. Using Landsat (30 m) data instead of MODIS may provide better accurate rice maps for smaller regions. Recent work has used the superior spectral and spatial resolution of Sentinel-2A MSI (Multispectral Instrument) data for mapping farms and other forms of land cover Utilizing high-resolution time-series imagery such as Quick Bird, IKONOS, and Rapid Eye, rice or crops have also been mapped. Because hyperspectral pictures are able to detect more

crop types, they can enhance crop mapping accuracy.

Rice and other land-cover types have been mapped using Decision Trees (DT),Support Vector Machines (SVM), Random Forests (RF)[6][7].In order to increase classification accuracy, more complicated techniques such as rotation forests (RoF) and adaptive network-based fuzzy inference systems (ANFIS) have been developed. Recent developments in the fields of image identification and signal processing have centered attention on deep learning[8][9]. Remote sensing applications, such as road-network extraction, vehicle detection, semantic segmentation and scenario classification benefit tremendously from the implementation of artificial neural networks (ANNs) in image processing[10][11]. When it comes to scenario categorization, an ANN can outperform traditional methods.

Using a convolutional window and local connections, ANN can extract spatial information from high-resolution land-use/-cover (LULC) categorization[12][13]. ANN and textural characteristics may also have benefits in LULC mapping such as agricultural categorization when utilizing moderate-resolution images like Landsat. ANN may be used for LULC mapping in two ways: with a pre-trained ANN or with a fully trained ANN. In the first method, learned knowledge from natural pictures is used for LULC classification [14]. The problem is that it needs RGB pictures, which are impracticable since multispectral images often comprise more than four channels (RGB, near-infrared, and another band).

Satellite remote sensing has been crucial in advancing rice and food security programs, with the community making great strides. Agro meteorology parameters such as temperature, precipitation, soil moisture and solar radiation are used widely in current Decision Support Tools (DSTs), which includes operational monitoring of the crops.

To examine the LULC changes processes, researchers most often utilize the remote sensing techniques, GIS and combination of models. The models which are based on equations, Markov chains, statistics and cellular models are mostly used methodologies. The Greater Bay Area is one of China's fastest-growing areas, and it has emerged as a global economic, educational, and technological crossroads. The GBA underwent a metamorphosis as a result of fast regional socioeconomic growth and urban dynamics, which had a significant influence on the geographical pattern of LULC alterations. We used the Modules for Land-Use Change Simulation (MOLUSCE) plugin inside QGIS software to model the spatiotemporal transition potential and future scenario of LULC in this work. Artificial neural networks (ANNs) and Monte Carlo cellular automata (CA) modelling techniques are among the algorithms included in the MOLUSCE plugin.

Human-environment connections may be better understood by looking at concepts like Land Use and

Land Cover (LULC) [15]. Human activity, such as farming, ranching, mining, and other forms of resource extraction, are all examples of what is referred to as land use. While Land Utilize refers to how people use Earth's surface for their own purposes (such as the effects of anthropogenic activities), land cover focuses on physical aspects of our Earth's surface, such as water, plant, as well as soil. Deforestation, urbanization, and agricultural intensification are all examples of human-caused LULC changes (LULCC), whereas natural disasters like droughts, floods, and wildfires are examples of natural LULC changes [16]. As a result, LULC data can help us understand how humans and the environment interact [17].The use of reliable LULC data has grown in recent years to support the implementation of policies linked to natural resource management and environmental issues such as food security, climate change, deforestation, and agricultural dynamics[18][19]. This emphasizes the importance of thorough mapping for long-term development [20][21].Large Earth Observation (EO) data sets are regularly used to get information about LULC and LULCC, and remote sensing satellite data are a great source for producing up-to-date LULC classifications [16]. For example, utilization of remotely sensed Time Series provides for the best understanding of study area and underlying process like greenhouse gas emissions, deforestation and agricultural growth [22]. LULC categorization, on the other hand, is a complicated procedure impacted by a variety of factors [23].Phenology measures, for example, have been frequently constructed from intermediate resolution data to better comprehend phenological cycles and uncover small differences across related classes [24]. MODIS attempts have yielded useful outcomes [25]. Information at finer spatial resolutions is necessary for various applications. In general, medium-resolution (Landsat-like, 10–30 m) sensors are the best for detecting most human contact, but low-resolution sensors are not effective for classification studies at the bigger scales, according to Chen and colleagues Comprehensive data on plant phenology may be gathered with the Landsat8 Operational Land Imager (L8/OLI) and the Sentinel-2 Multi Spectral Instrument (S2/MSI). There is now a new era for LULC and LULCC applications because of the rise in spatial resolution, open access rules, and systematic worldwide coverage of multi-source multi-temporal datasets with Landsat-like resolution. The two forerunners in moderate landscape mapping are Landsat and Sentinel [26]. L8/OLI and S2/MSI data are cost-effective methods for describing landscape processes at large scales because they share many technical properties [27]. The relevance of Landsat-8 and sentinel-2 data application for creating accurate mapping has been documented in the literature [28][29]. The data, however, have yet to be consolidated in order to give consistent recommendations on their impact on LULC classification methods, as well as to identify limits and viable techniques. To accomplish so, rather than relying on individual experience and skill, it is required to synthesis the collective knowledge on the subject

[30]. Systematic studies of remote sensing applications [31] have recently offered solid synthesis and scientific direction. None, however, concentrated on LULC categorization and LULCC detection using Landsat-8 and Sentinel-2 data.

Consequently, the primary objective of current research is to conduct an informative systematic review of papers that have been reviewed by peers and published in multiple journals from 2015, the years of MSI's to 2020, S2/launch on the usage of S2/MSI and L8/OLI spectral vegetation indices (VIs) and spectral bands to map the land use and land cover to monitor and identify changes in the landscape. This review covers the period from 2015 to 2020. Our specific objectives are as follows: (1) to provide scientific based guidelines as well as new insights for the future research by summing up scientific advancements for LULC detection and LULCC classification, as well as existing limitations and issues; and (2) to provide scientific based guidelines and new insights for the future research by summing up scientific advances for LULC detection and LULCC classification, as well as existing issues and limitations.

1.1 Landsat 8 /OLI Features

They are publicly accessible, interoperable, and capable of monitoring huge surfaces, S2/MSI and L8/OLI data are used as input for the LULC and LULCC systems all around the globe.

These mentioned sources are positioned in the sun-synchronous orbits and perform identical spectral, spatial, and angular observations.

Table 1 Characteristics of L8/OLI

Spectral Band	L8/ OLI Central Wavelengths
Coastal/Aerosol	442.9 nm (30 m)
Blue	482 nm (30 m)
Green	561.4 nm (30 m)
Red	654.6 nm (30 m)
NIR	864.7 nm (30 m)
SWIR	1608.9 nm (30 m), 2200.7 nm (30 m)
Panchromatic	589.5 nm (15 m)
Cirrus	1373.4 nm (30 m)

In addition to the Thermal Infrared Sensor (TIRS) and the Operational Land Imager (OLI), NASA and the United States Geological Survey's L8 satellite carries two sensors: the OLI (nine bands and 30 m of the geographical resolution) and the TIR (two bands and 100 m of the spatial resolution). Both the radiometric and temporal resolutions are set at 16 bits. Each occupies a certain amount of space. It takes 185 and 180 kilo meters to get there. As part of the Copernicus Earth Observation program of the European Union's Europe Space Agency (ESA), two satellites (S2A/MSI and S2B/MSI) were deployed in 2015 and 2017. A 13-band sensor with a resolution of 10 to 60 meters in the SWIR ranges are installed on both S2 satellites. Sentinel-2 satellite provide data with a 5-days return cycle, sweep width of 290 km and 16 bits of the radiometric resolution. With the S2/MSI mission's spectrum capabilities, it provides new mapping choices. This range may be utilized to determine band ratio and construct a variety of indices. They can be helpful for identification and LULC categorization. Landsat's 16-day return duration and spatial and spectral resolution issues may lead to inaccurate results for LULC and LULCC analyses, however these benefits may outweigh these drawbacks. Landsat-8 and Sentinel-2 satellite images data provide a revisit period of around three days, enabling landscape monitoring with the clear observations in selected areas.

1.2 Statement of Problem

Existing traditional agricultural systems rely heavily on sparse ground-survey data, but multi-spectral as well as multi-temporal remote sensing pictures have shown to be effective instruments for assisting vulnerable systems by properly monitoring and predicting crop yields prior to harvest.
We need a simple, scale able and inexpensive method for timely forecasting rice yield across a vast area with publicly accessible data, which has the potential to be used to locations with infrequently observed data as well as globally to estimate crop yields.

- Rice genotype classification
- Rice genotype classification will help to identify the best varieties in terms of yield.
- LULC will also help to identify the total area where rice is grown.

1.3 Objectives

- The goal of this work is to look at machine learning architectures that have previously been used to identify LULC in satellite photos in order to increase detection performance and detect vegetation.
- The goal of this work is to look at machine learning architectures that have previously been used to identify LULC in satellite photos in order to increase detection performance and detect vegetation.
- To develop model for identification of rice varieties using Land use Land cover Classification.

- To evaluate the performance of the ANN.
- To map the results of ANN.

2. Literature Review

China and the rest of the world's food supply have long been a source of concern [32][33]. Rice, a staple meal in China, is grown in large quantities [34]. In other locations, however, rice production has lately been hampered by difficulties. With a rising population comes an increased need for rice, yet the acreage of rice fields has decreased due to urbanization, making it more difficult to meet that need. Rice production is also affected by environmental deterioration and natural disasters, such as floods and droughts. Government decisions need quick and accurate assessments of rice output, which may be obtained via the monitoring of rice-producing fields with high spatial–temporal resolution. Paddy rice farming has a significant impact on food and water security, greenhouse gas emissions and the health of human if accurately and timely rice paddy field maps with the fine spatial resolution are available. Both high time resolution and coarse spatial resolution optical images were used to create rice paddy field maps (e.g., Moderate Resolution Imaging Spectroradiometer) and high spatial resolution and low temporal resolution optical pictures (e.g. Landsat TM/ETM+). For the sake of rice paddy field mapping at precise spatial resolutions, data availability and image-based methods hindered accuracy and efficiency.

The ability to generate up-to-date, accurate land use/land cover (LULC) maps, as a result of ecosystem and land use changes, has become more practical because to advances in remote sensing techniques and expanded availability to satellite data [35]. When it comes to picking an algorithm, many people have difficulty. Site circumstances, available data, and spectral similarity across classes all factor into the algorithm selection process.

As Landsat 8 and Sentinel-2 multispectral instruments have recently been used to collect data on land use and land cover, new possibilities for remote sensing analysis have emerged. By combining various data sets, researchers may better classify landscapes and their underlying processes, such as deforestation and agricultural development, while also detecting changes in those processes [36].

It has been difficult to monitor large-scale rice farming due to poor radar coverage, low spatial and temporal resolutions of optical sensors, and a lack of systematic or open access radar. Sentinel-1 C-band data with a dense time series and a moderate geographic resolution, freely available, opens up new possibilities for agricultural monitoring. It's particularly relevant in rice-growing regions like South and Southeast Asia, because the rainy seasons, when thick cloud cover is prevalent, are the most important times for rice cultivation. Sentinel-1A Interferometric Wide images (632) from a time

series were used in this study to map Myanmar's rice expanse, crop calendar, flooding, and cropping intensity. Sentinel-1, Landsat-8 OLI, and PALSAR-2 were combined and categorized using a random forest method to provide an updated (2015) land use and land cover map. Sentinel-1 data were subsequently used to conduct phenological analysis of rice information over the whole country of Myanmar.

Climate change, which includes variations in temperature, precipitation, and CO2 levels, may have a negative impact on crop production [37]. Climate models can forecast regional temperature changes more accurately than they do regional precipitation changes, making temperature rises the most likely to have a negative impact on agricultural yields [38]. The average annual temperature has increased by 1°C over the previous century in places where wheat, rice, maize, and soybeans are cultivated and is expected to climb considerably more over the next century if greenhouse gas emissions rise any further (Nelson et al., 2010). Because of this, it is imperative that the impacts of temperature rise on global crop yields, including any geographical variability, be measured to identify the threat of world food security and then develop appropriate adaptation plans to feed a rising global population [39]. In developing and emerging countries, climate change has the greatest influence on socioeconomic [40]. Climate change's most evident expression has been extreme warming (Asseng et al., n.d.). Global temperatures are quickly increasing, and they might climb by 20°C to 60°C by the end of the twenty-first century [41].

An ANN technique was utilized to identify 1779 Italian rice varieties, utilizing surveyed measures that are typically measured for the commercial categorization of a product, such as grain size and color. Based on Kohonen network, it was possible to differentiate classes that were indistinguishable in Principal Component Analysis (PCA) space, compared to the traditional PCA. According to classification and prediction, the best CP-ANN properly predicted more than 90% of test set samples [42].

To keep food production on schedule and analyses the influence of climate change on rice production, industry stakeholders need to conduct regular monitoring and mapping of rice (Oryza Sativa) development stages. It has been common practice in Indonesia to conduct expensive field surveys to check rice growth. The approach proposed in this study uses satellite images and machine learning to extract multi-temporal rice phenology (vegetative, reproductive, and ripening) and bare land mapping. We trained the models using a wealth of ground validation data gathered between 2014 and 2016. Pre-installed cameras in Indonesia were used to gather this ground validation data. A total of five machine learning techniques were employed to categorize rice development stages and barren land using random forest (RF), support vector machine (SVM), and artificial neural networks (ANN)

[43].

It is possible to fill up the data gaps with trustworthy spatial data from regional to global sizes using remote sensing technologies. Sentinel satellite missions [44] are examples of Earth observation missions that monitor Earth's surface on a regular basis with a variety of spectral and spatial resolutions in order to better understand and address food security issues [45]. There have since been a number of remote sensing investigations on rice phenology in various environments, including irrigated and rain-fed regions. Different sensors have been suggested for the detection of rice phenology using a variety of broad and narrow-band vegetation indices, such as the normalized difference vegetation index (NDVI) and the enhanced vegetation index (EVI). A root-mean-square error (RMSE) of 12.1 days on planting date was achieved using MODIS data with 500 m resolution and a wavelet filter, according to [46]. Rice transplanting stages may be detected using EVI and Land Surface Water Index (LSWI) generated from MODIS using 8-day composite pictures, according to Xiao and colleagues [47]. While their results are close to those of a local ground truth database, their precision dwindled across mountainous terrain, as seen by their lower accuracy. Because the Landsat-8 OLI sensor has increased performance in radiometric and spectral resolutions, it is capable of mapping paddy fields with more precision than MODIS and Landsat-7 in subtropical areas. Even in tropical and subtropical regions, fast land use change caused by natural catastrophes (such as tropical cyclones, earthquakes, landslides, floods, and volcanic eruptions) and changing weather, as well as urbanization and recurring cloud cover, influence Landsat-8 OLI accuracy[48]. Radar imaging, such as Synthetic Aperture Radar, Sentinel-1A, and RADARSAT was commonly utilized to overcome weather restrictions (e.g. cloud and shadow cover). Access to RADARSAT, on the other hand, might be an expensive burden for nations in emerging stages to deploy. As a result of this, the analysis necessitates expensive and time-consuming clustering of clean and time-series data by a qualified individual or utilizing existing knowledge of the subject region.

Optical and radar data may be used to map crop kinds and estimate biophysical characteristics, particularly with the Copernicus program's unparalleled volume of free Sentinel data. It is possible to monitor crops every five or ten days using these databases, which are guaranteed for decades. Understanding the temporal changes of the remote sensing signal of various crops in a particular location is essential before creating operational monitoring approaches. SAR and multi-temporal hyperspectral pictures recorded at varying time intervals may both be used for automatic change detection studies in remote sensing technology [49]. These photos are compared and a categorization is made between the modified and unaffected regions. Noises in the RS pictures, on the other hand, weaken current algorithms[50]. Convolutional neural networks (CNNs) are used in the deep learning

framework to recognize burned regions automatically utilizing every fresh SAR picture obtained during the wildfires and to describe the temporal backscatter fluctuations using all existing pre-fire SAR time series. For the Elephant Hill Fire in British Columbia, Canada; the Camp Fire in the United States of America; and the Chuckegg Creek Fire in Alberta, Canada, Sentinel-1 SAR backscatter was able to identify wildfires and document their temporal evolution. The CNN-based deep learning architecture can better discriminate charred regions than the standard log-ratio operator. Spaceborne SAR time series with deep learning may play a big role in near real-time wildfire monitoring when the RADARSAT Constellation Missions are launched in 2019 and SAR CubeSat constellations are launched [51].

Ensemble-based techniques have emerged as the most widely used and most effective methods for classifying land cover across several sensors and time scales in the last few years. Deep learning (DL) and machine learning (ML) [52]. The SVM is outperformed by several approaches [53]. Deep learning is a sophisticated machine learning technology that may be used to solve a broad variety of image processing and computer vision challenges, as well as natural language processing tasks. When dealing with large data, it is important to utilize as much data as possible in order to replicate human vision and offer meaningful information. It is easy to find picture categorization models, frameworks, and reference imagery databases to test against. There has been an increase in the use of DL for RS image processing during the last several years [54]. A number of different land cover categories, such as roads and buildings, may be extracted from satellite photos using DL, including optical (hyperspectral and multispectral imaging), as well as radar images. For RS tasks, convolutional neural networks (CNNs), deep belief networks (DBNs), and recurrent neural networks (RNNs) with long short-term memory models have previously been tested [55]. Classification, such as land cover or object identification, is often performed on a single date picture in most research using DL for RS, but this is not always the case. In order to properly identify certain land cover classes, such as crop kinds, multitemporal photos are often necessary. A large-scale crop map is created using many remote sensing images. For the creation of the f phenological feature set, we used harmonic analysis to extract harmonic phenological features and harmonic backscattering features from images taken by Landsat-8 and Sentinel-2, and then combined them with spectral features from both those satellites' images and those taken by Sentinel-1 to get the normalized difference vegetation index time-series.

The following issues must be addressed when utilizing ANN for large-scale crop mapping using multitemporal satellite images. Pixels in a satellite picture are first and foremost physical. This is because the backscatter intensity and phase of the backscatter in various polarizations are different

for each pixel of the spaceborne SAR imaging than for each pixel of the optical imagery, and each pixel of the optical imagery might be affected by clouds and shadows. Both data sets are multitemporal, but their spatial resolutions are quite different. There are several reasons why multitemporal multisensory satellite data must be fused in ML implementation for land cover and crop classification.

3. Material and Methods/Model and Equations/Modelling

There are different material and methods used to conduct the research as described below.

3.1 General Overview of Architecture

For the categorization of crop kinds using multitemporal satellite images, a four-step architecture has been suggested. 1)Preprocessing, 2) postprocessing 3) Supervised classification and 4) Geospatial analysis are the four stages (Fig. 2).

Optical satellite images may be polluted by clouds and shadows, missing values in the picture must be dealt with. Because wide range of classifiers only take valid pixel values ass input, a preprocessing step to impute (or fill gaps) missing data is required. This method is carried out at the architecture's level I. The following phase, which is the focus of this letter, is supervised categorization (level II). RF architecture is proposed. Levels III and IV are for enhancing the categorization map using accessible geographical layers and creating high-level deliverables. Fig. 1 shows the proposed methodology.

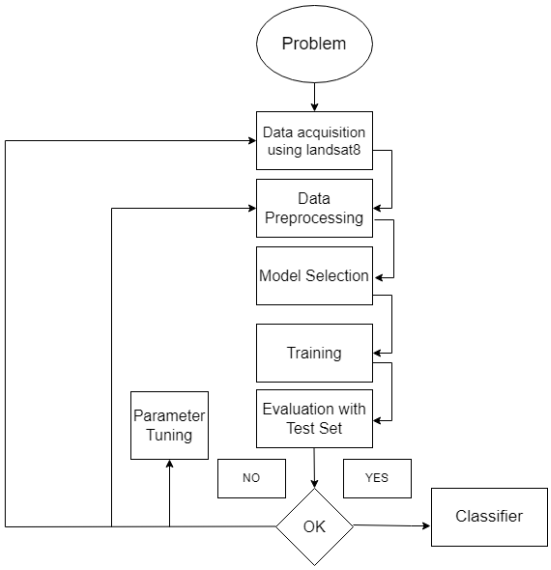

Fig.1 Proposed Methodology

Crop area estimate and crop rotation area estimation are examples of the latter. The next sections go through each of these architectural levels in further depth.

3.2 Reprocessing

We use self-organizing Kohonen maps (SOMs) for optical image segmentation and subsequent missing data restoration in a time-series of satellite imagery for preprocessing. SOMs are trained independently for each spectral band using non-missing data. Missing values are recovered usinga unique algorithm that replaces the missing components of the input sample with the weight coefficients of the neuron. The number of cloud-free scenes accessible for each pixel from optical images is determined, and these two layers are utilized for a more advanced postprocessing approach (at level III) to enhance the resultant classification map.

3.3 Image Classification

Using a variety of satellite datasets, this research compares the map accuracies of the SVM and RF classification algorithms employed in paddy rice land-cover studies. Supervised learning classifier SVM doesn't need any parameters or distributions to work. The various training samples in an input space are projected onto a high-dimensional space using a kernel function that enables classes to be separated. It has been stated that the RF method can handle larger training sets than typical classifiers in order to achieve map accuracies that are greater than traditional classifiers.

3.4 Post processing and Geospatial Analysis

We created numerous filtering methods based on available information on the quality of input data and field boundaries, such as parcels, to enhance the quality of the final map. These filters use a pixel-based categorization map and custom rules to account for multiple plots (fields) inside a parcel. We were able to create a clear parcel-based categorization map as a consequence. Data fusion using multisource heterogeneous information, such as statistical data, vector geospatial data, socioeconomic data, and so on, is provided at the ultimate level of data processing. The Below diagram explain four steps I) Data collection or sample points II) Application of Artificial neural network giving band information III) Mapping the output IV) Area calculation.

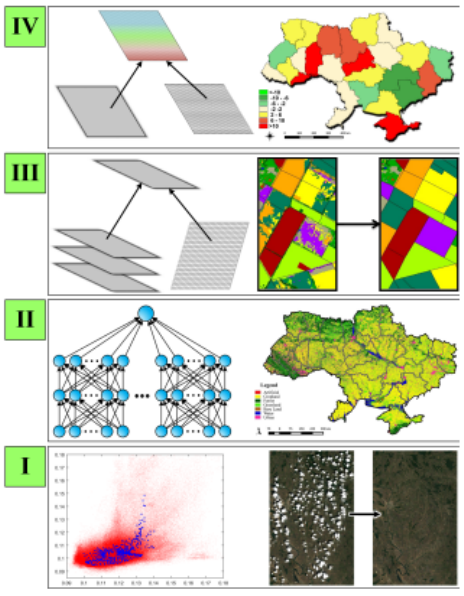

Fig.2 Four-level hierarchical ML model for satellite data classification

3.5 Study Area

We use pictures taken by the Landsat-8 satellite to solve the issue of land cover and crop categorization in the Rahim Yar Khan area of Pakistan. Major agricultural crop (rice) is among the classification studied. It covers a broad area with a wide range of land cover types and agricultural crops. The area is large enough to be regarded indicative for the spread of technology across the nation. The chilly season starts in December and lasts until the end of April.

3.6 Data Sample

Table 2 515 Rice Variety

B2	B3	B4	B5	B6	B7	B8	B8A	B11	B12	datetime
1042	1228	1386	1609	1831	2018	2082	2101	2547	2355	30-05-2021 6:00
1130	1368	1510	1769	2105	2258	2216	2409	2560	2230	30-05-2021 6:00
1128	1290	1512	1696	2003	2223	2170	2331	2522	2180	30-05-2021 6:00
1042	1236	1390	1679	1918	2095	1952	2182	2519	2325	30-05-2021 6:00
993	1218	1318	1615	1919	2091	2104	2261	2595	2164	30-05-2021 6:00

Table 3 Laal86 Rice Variety

B2	B3	B4	B5	B6	B7	B8	B8A	B11	B12	datetime
1334	1628	1908	2081	2407	2506	2408	2694	2796	2501	20-05-2021 6:00
1106	1354	1540	1888	2140	2329	2148	2402	2544	2284	20-05-2021 6:00
1232	1538	1746	1916	2108	2310	2372	2359	2493	2212	20-05-2021 6:00
1296	1566	1874	1888	2140	2329	2410	2402	2544	2284	20-05-2021 6:00
1156	1454	1654	1929	2240	2442	2414	2509	2578	2169	20-05-2021 6:00

Table 4 Super Rice Variety

B2	B3	B4	B5	B6	B7	B8	B8A	B11	B12	datetime
1296	1664	1644	1935	2293	2465	2414	2556	2362	1977	11-06-2021 5:50
1314	1662	1672	2018	2751	2959	2644	3042	2671	2092	11-06-2021 5:50
1146	1426	1372	1935	2293	2465	2258	2556	2362	1977	11-06-2021 5:50
1484	1818	1980	2106	2479	2603	2468	2682	2680	2294	11-06-2021 5:50
1202	1516	1522	1867	2506	2696	2460	2817	2396	1848	11-06-2021 5:50

Table 5 White86 Rice Variety

B2	B3	B4	B5	B6	B7	B8	B8A	B11	B12	datetime
1150	1462	1582	1903	2434	2670	2692	2798	2968	2441	22-05-2021 5:50
1086	1338	1542	1739	2265	2444	2448	2577	2747	2170	22-05-2021 5:50
1128	1396	1636	1902	2168	2299	2592	2389	2326	1999	22-05-2021 5:50
1086	1338	1542	1739	2265	2444	2448	2577	2747	2170	22-05-2021 5:50
1136	1426	1622	2034	2340	2559	2702	2649	2784	2387	22-05-2021 5:50

3.7 Feature Sets

Multi-temporal characteristics based on crop phenology were created in order to investigate the potential of optical images from Sentinel-8 to discriminate land cover classes and to pick the most important features for increasing classification accuracy. Crop mapping input data were examined using a variety of feature sets and optical feature combinations. The classification performance or uniqueness of six spectral indices was considered while selecting them from the literature. The features were extracted using ENVI and SNAP software. In Fig. 3, we used the Features sets, features and numbers of features for crop mapping. We utilized the 400 samples in training for each class400 X 4. And 20% of the sample data we used for the testing of model.

No.	Feature Sets	Features	Number of Features
1	Spectral Band (SB)	Multi-temporal spectral bands	80 (8 × 10 bands)
2	Spectral Index (SI)	Multi-temporal NDVI [38], EVI [39], ARVI [40], RVI [41], NDWI [42], IRECI [43]	48 (8 × 6 index)
3	Texture (T)	Multi-temporal local moments (mean, variance), Haralik (CON, DIS, HOM, ENE, ENT, COR) [37] in each spectral band	640 (8 × 10 bands × 8 textures)
4	Variation of Spectral Index (VSI)	Multi-temporal VSI of NDVI, EVI, ARVI, RVI, NDWI, IRECI	48 (8 × 6 index)
5	Combination of FS 1, 3 (SB-T)		720
6	Combination of FS 3, 4 (T-VSI)		688
7	Combination of FS 1, 2, and 3 (SB-SI-T)		768
8	Combination of FS 1, 2, and 4 (SB-SI-VSI)		176

Fig. 3 Different feature sets and combinations of optical features for crop mapping

3.8 Machine Learning

Machine learning is an AI branch that focuses on the creation of computer programs that have data access by providing a system with the capacity to learn and improve automatically. Finding patterns in a database without human interaction. Machine learning algorithms are further classed as Supervised, Unsupervised, and Semi-Supervised; all of these learning approaches are employed in various applications. Machine learning is a subset of Artificial Intelligence in which computers automatically learn from their operations and fine-tune themselves to provide better results.

The first one thing that is comes to mind for the most of people when they hear the word "artificial intelligence" is a machine. Based on the idea that human intellect may be characterized in a manner that machines can simply duplicate it and perform tasks is known as "artificial intelligence. Fig. 4 consist of two phases. Phase 1 shows that how training data will perform and how many steps involved in it and Phase 2 shows that how predict the model and shows the predicted data.

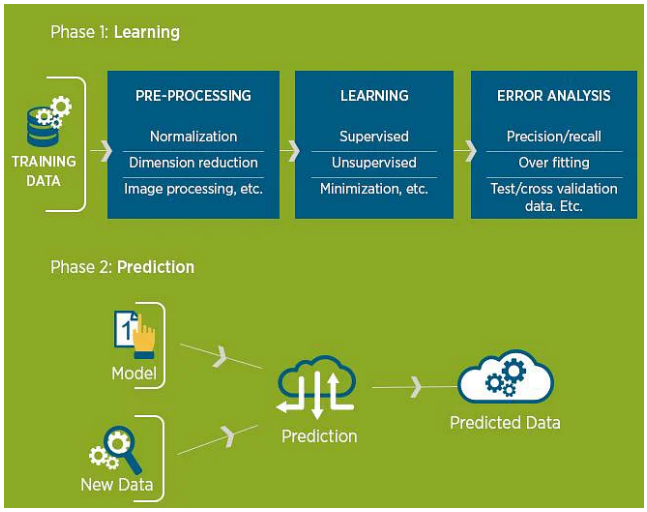

Fig.4 Machine Learning Process

3.8.1 Supervised Machine Learning

Data is labeled and categorized, supervised learning methods are applied. The algorithms learn from earlier inputted data, known as training data, and utilize this analysis to predict future occurrences of any new data within the established categories.

3.8.2 Unsupervised Machine Learning

Unsupervised learning techniques are utilized when we are unsure of the eventual outputs and do not have access to categorization or labeled outputs. These algorithms investigate and develop a function to describe entirely unlabeled and concealed patterns. As a result, there is no proper output; instead, it analyses the data to reveal undiscovered structures in unlabeled data.

3.8.3 Semi Supervised Machine Learning

These algorithms often process labeled and unlabeled data, with the unlabeled data quantity being greater than the labeled data amount. These models have been shown to increase learning accuracy in systems. In an ideal world, all data would be organized and categorized before entering a system.

3.9 Validation and Accuracy Assessment

The observation regarding the reliance on remote sensing data without sufficient ground truth data for validation is a valid concern while remote sensing data is a powerful and invaluable for large-scale analysis, indeed has limitations, particularly when it comes to validation against on-the-ground realities. However, several factors were considered in this study to mitigate the potential impact of

this limitation.

First, the study employed a rigorous accuracy assessment protocol using existing ground truth data from previous studies and publicly available datasets. While direct, contemporary ground truth data collection was not feasible within the scope and resources of this research, the use of well-established reference datasets provided a reliable means to validate the remote sensing classifications. These datasets, which include historical land cover maps, agricultural census data, and other relevant sources, have been widely used in the literature and are considered robust for validation purposes. Secondly, advanced remote sensing techniques, such as the use of high-resolution satellite imagery and machine learning algorithms, were implemented to enhance the accuracy of land use and land cover (LULC) classification. These methods allow for the extraction of fine-scale features that closely approximate ground conditions, reducing the reliance on extensive ground truth data. The integration of machine learning models, such as Random Forest and Support Vector Machines, provided a significant improvement in classification accuracy, as these models are particularly adept at handling the complexities of remote sensing data.

The study also incorporated cross-validation techniques to ensure the robustness of the results. By splitting the dataset into training and testing subsets, the models were evaluated on their ability to generalize beyond the initial training data. This approach helped to identify potential overfitting and ensured that the models produced reliable and accurate classifications, even in the absence of extensive ground truth data.

3.10 LULC

The vast majority of usable land today is being put to use in a way that directly impacts human needs. Aside from the intense usage of the land, the land is also changing and altering with time. What was farmland 10 years ago is now likely to be urban land. A plantation has likely taken over what was once forest land. As land use and land cover (LULC) change at such a fast pace, it's become necessary to quantify these shifts in figures and maps so that we may better comprehend and use this data.

Though they're commonly used interchangeably, land usage and land cover signify quite different things. Activities that take place on a parcel of land are known as "land usage." A land cover, on the other hand, refers to the kind of vegetation that grows on the ground.

3.10.1 LULC change detection

Land use and land cover change (LULC) is a very complicated process that can take many different shapes and progress at varying rates and magnitudes. Governments around the world have devoted

entire bureaus to tracking and analyzing these changes. Studies on LULC change detection are typically conducted in conjunction with other research on a related issue. The National Land Cover Database (NLC) of South Africa, for instance, was created using geo rectified, single-data, 1:250,000 scale LANDSAT Thematic Mapper (TM) satellite imagery from the years 1994–1955. The first significant attempt to map the LULC of India was made as part of the LULC 2005-ISRO Geosphere-Biosphere Program LULC Dynamics Project. Using multi-temporal AWiFS datasets, it created a 1:250,000 scale map of the entire nation. The majority of LULC studies use images from satellites like Landsat (TM), Carto sat, LISS series, and others.

3.10.2 Integration of Additional Satellite Data Sources

The current study primarily utilizes Landsat-8 imagery, which has been effective in mapping rice crops within the specific region. However, integrating additional satellite data sources like MODIS could indeed enhance the robustness of the models by providing higher temporal resolution and complementary spectral information. The fusion of data from multiple satellites can improve classification accuracy, particularly in areas with frequent cloud cover or other data limitations. Future research could explore combining MODIS data with Landsat-8 to achieve a more comprehensive temporal analysis and reduce gaps caused by missing data.

3.11 Structure of ANN

Multispectral assessment of satellite images data has been utilized to create thematic LULC inventories for a variety of products such as crop characterization, urban planning and forest ecosystem categorization. ANNs were initially intended to be Tools for image analysis and input evaluation that mimic the brain's neuronal storing and cognitive functionalities. ANN techniques offer a particular, they have a plus over scientific classification techniques in that they are non-parametric and require minimal or no prior information of the input feature estimation method. Based on ERDAS IMAGINE 9.0, this categorization approach is more viable and computationally efficient. Our automatic ANN classification system was made up of a supervised multilayer perceptron (MLP) network module and Kohonen's self-organizing mapping (SOM) neural network module. While several ANN methods have been utilized in a variety of LULC classification applications using remotely sensed data, supervised multilayer perceptron (MLP) and unsupervised SOM neural networks are the most often used ones. Fig. 5 depicts MLP networks, which generally consist of one input layer, one or more hidden layers, and one output layer, are often trained using the supervised back propagation (BP) technique.

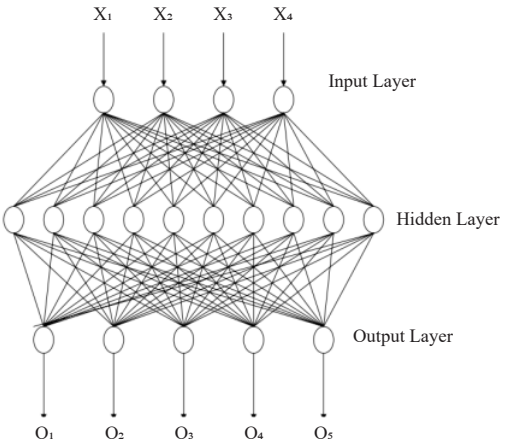

Fig. 5 An example structure of Neural network

Fig. 6 depicts the Kohonen's artificial neural network model. Developed as an unsupervised clustering artificial neural network (ANN), generates a one- or two-dimensional map of the associations among input data patterns.

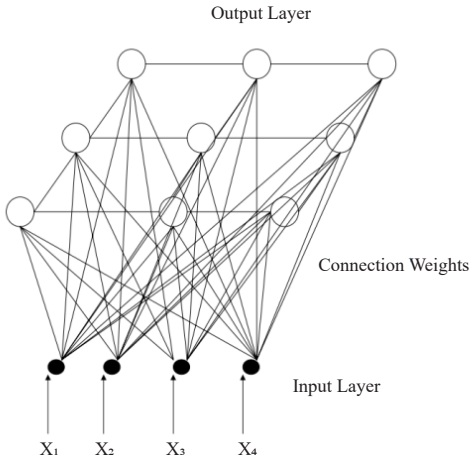

Fig. 6 The structure of Kohonen's Self-Organization Mapping neural network.

3.11.1 Parameter Selection

The network configuration, ANN involves the selection of a set of characteristics for the training procedure, including the learning rate, dropout rate, batch size, and the number of training epochs. Selecting the ideal set of input values is difficult and necessitates preliminary research. A grid search was used to find the best arrangement for carrying out all trials by using the parameter and selected value (Table 6).

Table 6 Training parameters

Parameter	Parameter
Starting Learning Rate	1.5
End Learning Rate	0.15
Decaying Learning Rate	True
No. of Layers	3
Momentum	0.08

3.11.2 Training and Testing of ANN

The amount of training parameters varies depending on the network and method. The following MLP network parameters were necessary in our investigation:

1) Starting learning rate,
2) End learning rate,
3) Momentum
4) Epochs.

3.11.3 Neural Network Classification and Discussions

Using USGS tools, various picture subsets were initially picked from image for each class. We wanted to collect picture subsets from both homogenous and diverse locations. Image subsets were allocated to categories with a lot of spectral variation within the class, such the urban and agricultural sectors. The chosen photo subsets were processed using the feature transformation sub-modules of the neural classification system. The learning and evaluating patterns were extracted from the picture subsets using this sub-module, coded, and stored as testing and training pattern data for each class. Each sampled pattern's appropriate class label was provided via MLP classification. In this application, 420 learning pixels and 45 evaluating pixels were picked for each of the six classes, totaling 3360 learning pixels and 360 evaluating pixels. During training, the network was only subjected to the 3360 training patterns.

Many MLP tests with various hidden nodes and training settings. An error file was created after each iteration to capture the training and testing failures. The appropriate network design and training parameters were found using these error files. The ideal MLP network architecture in this scenario was discovered to be a single layer network with 15 hidden nodes. The best MLP training was obtained when the following parameters were used: 1) 15,000 epochs, 2) 1.5 starting learning rate, 3)

0.05 end learning rate 4) momentum (0.08). The well-trained MLP network was fed into the network generalization sub-module and utilized to categories the TM picture into the six LU/LC classes depicted in Figure 7.

3.12 Performance Evaluation

3.12.1 Accuracy

Classification performance is measured using either accuracy or its inverse error rate. Accuracy is defined as the percentage of examples that were correctly classified, while error rate is the percentage of examples that were incorrectly classified.

$$\text{Accuracy} = \frac{TP+TN}{TP+FN+TN+FP} \quad (1)$$

3.12.2 Precision &Recall

When it comes to evaluating text mining performance, there are two metrics in wide use: precision and recall. Precision is the number of positive examples correctly labeled divided by the total number of instances in which those positive examples are encountered. Recall is the number of positive examples that are actually found and can be distinguished from all other instances. The following formulas illustrate this concept.

$$\text{Precision} = \frac{TP}{TP+FP} \quad (2)$$

$$\text{Recall} = \frac{TP}{TP+FN} \quad (3)$$

4 Results and Discussion

This section contains the results of using the neural networks approach for LULC mapping. The analysis was carried out in three stages: pre-processing, ANN training, and LULC mapping. During the applications, Landsat 8 images were used. Sheikh Pura in Pakistan is the location of the research. The ANN classifier was created using the TensorFlow library. The ANN classifier was trained until it achieved the lowest possible error. Based on the confusion matrix measure, the accuracy we achieved using NN o remotely sensed training data is 98%, while accuracy of testing data is 91%. The best performance was obtained following a series of trials with various training functions or varying numbers of neurons in the hidden layers.

The classification results demonstrated that the trained MLP network generalized well. The previously mentioned cross-validation training strategy was beneficial in terms of preventing over-fitting.

In general, ANN classifier performance accuracy is good in classes with a large area compared to low performance in classes with small areas. According to the regional level of study, the classifier's performance is fairly good. Fig. 7 shows that LULC map image used to classify Landsat 8 image based on TensorFlow and ANN classifier.

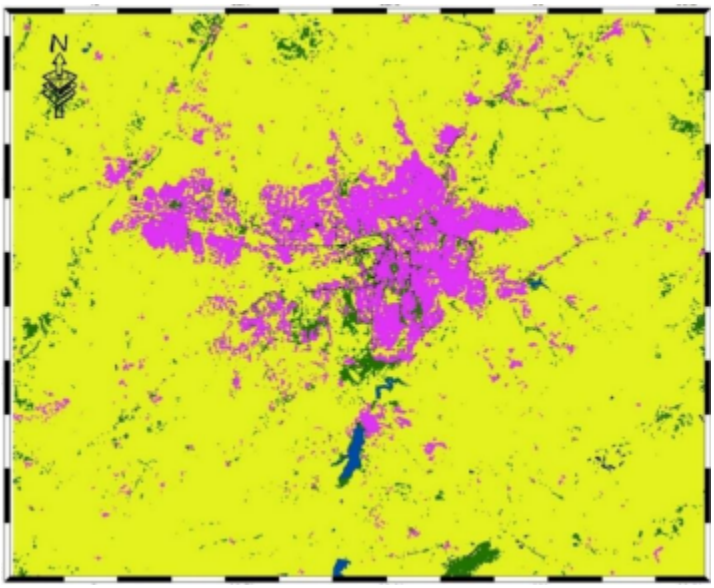

Fig.7: LULC MAP

The following are some key findings from this study:

An automated Identification techniques system was created and demonstrated to be appropriate for land use / cover mapping using satellite data, particularly when the pattern of the training dataset is atypical.

This research offered a good study to validate the automated ANN's superior classification skills over other systems for LULC applications. Based on the findings of this study, the supervised MLP networks can be used in typical Land use land cover mapping applications to achieves better classification results, and unsupervised MLP model can be used to provide aid in analyzing the satellite images data and the features of remotely sensed data.

MLP is extremely helpful in the less time-consuming and crucial work of collecting and evaluating remotely sensed training data for classification of complicated LULC.

Super rice, 515, laal86, white86, duckweed, open water, buildings, and others were among the several land-cover types that were surveyed. The first Lansat-8 photograph was taken in June of that year. Backscatter was remained high in rice fields since they were either occupied by other crops or were in the process of being prepared. Paddy rice A is the name given to the second accessible picture in July (2021) that shows a decrease in backscatter due to floods or freshly replanted rice crops. Paddy rice B refers to rice fields inundated after June 18, 2021, whose decline in backscatter was only noticed in the third available photograph (July 1). After the third accessible photograph, the backscatter of rice subtypes is consistent with one another (25 July). However, in June of 2021, two photos were made accessible (01 June and 08 June). More pixels of Paddy A were captured in 2021 because of the wider window available for Paddy A capture. The relative efficacy of ANN algorithms in rice mapping utilizing single optical data throughout and between seasons was proven using pixel-based accuracy evaluation. Each dataset yielded similar results from ANN. The linear correlation between VH and VV polarizations may be inferred from the backscatter patterns' temporal consistency. The rise in satellite observations in 2021 is to blame for this (Landsat-8) when compared to other datasets. This is in line with the results obtained by combining VH and SI.

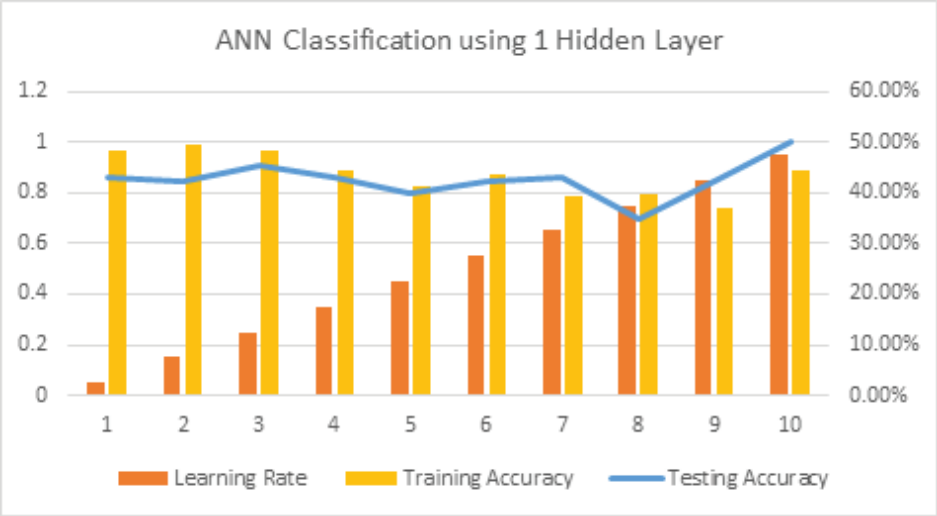

Fig. 8: ANN Classification using 1 Hidden Layer

Fig. 8 shows the learning rate, training accuracy and testing accuracy on USGS data set using 1 hidden layer. By using ANN classifier achieved maximum 98.69% training accuracy, 50% testing accuracy.

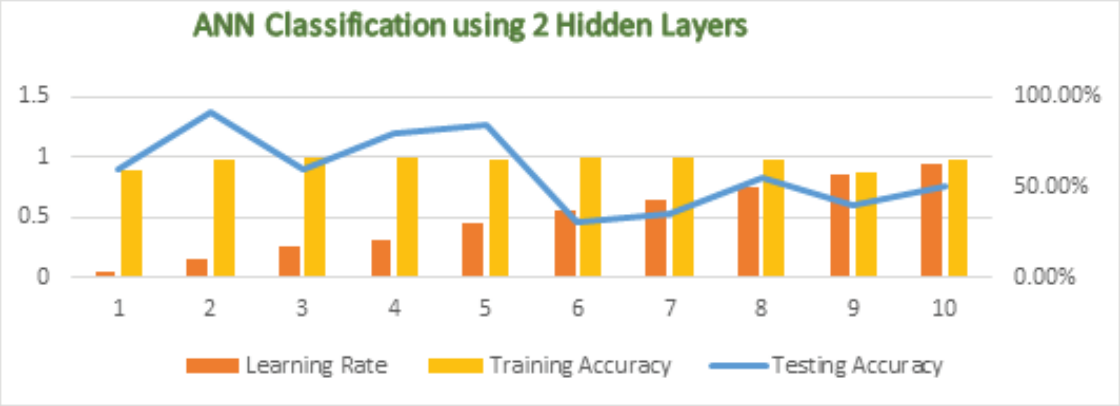

Fig. 9: ANN Classification using 2 Hidden Layers

Fig. 9 shows the learning rate, training accuracy and testing accuracy on USGS data set using 2 hidden layers. By using ANN classifier achieved maximum 99% training accuracy and 91% testing accuracy.

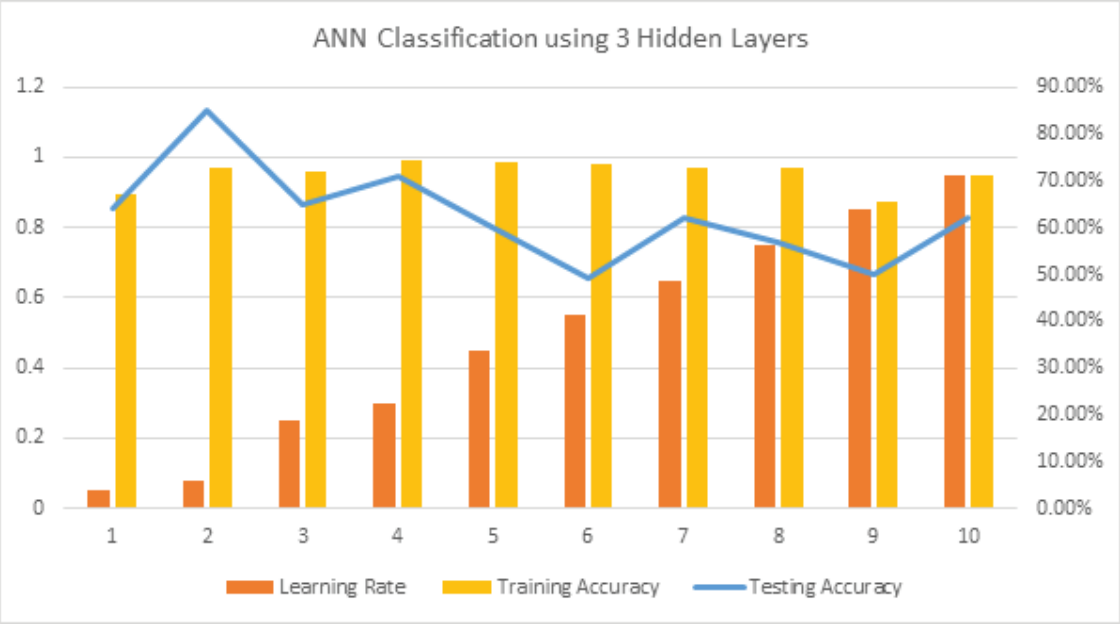

Fig.10 ANN Classification using 3 Hidden Layers

Fig. 10 shows the learning rate, training accuracy and testing accuracy on USGS data set using 3 hidden layers. By using ANN classifier achieved maximum 99.23% training accuracy and 85% testing accuracy.

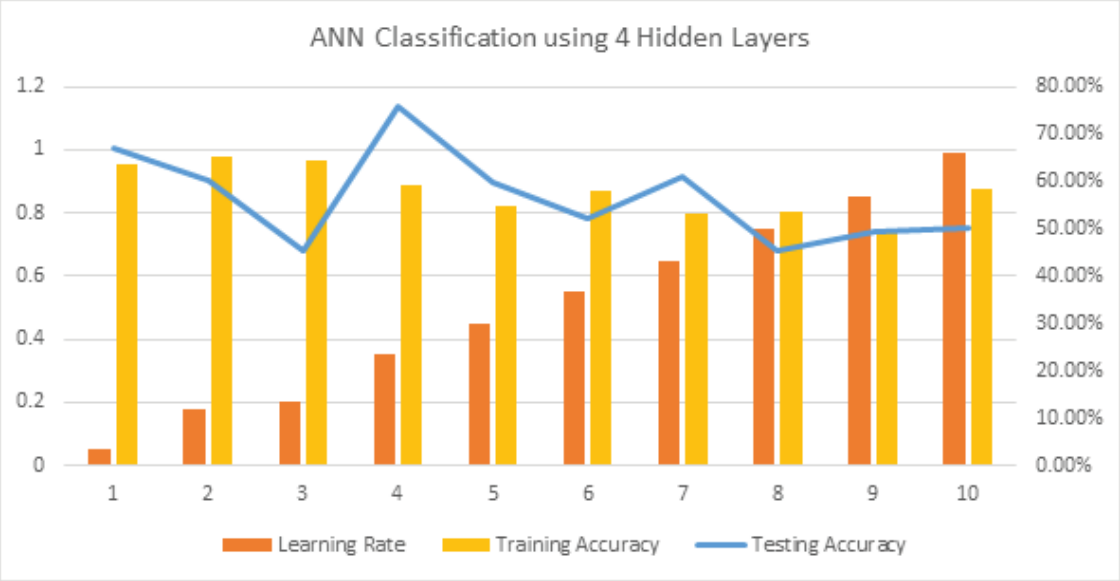

Fig.11 ANN Classification using 4 Hidden Layers

Fig. 11 shows the learning rate, training accuracy and testing accuracy on USGS data set using 4 hidden layers. By using ANN classifier achieved maximum 97.69% training accuracy and 75.87%testing accuracy.

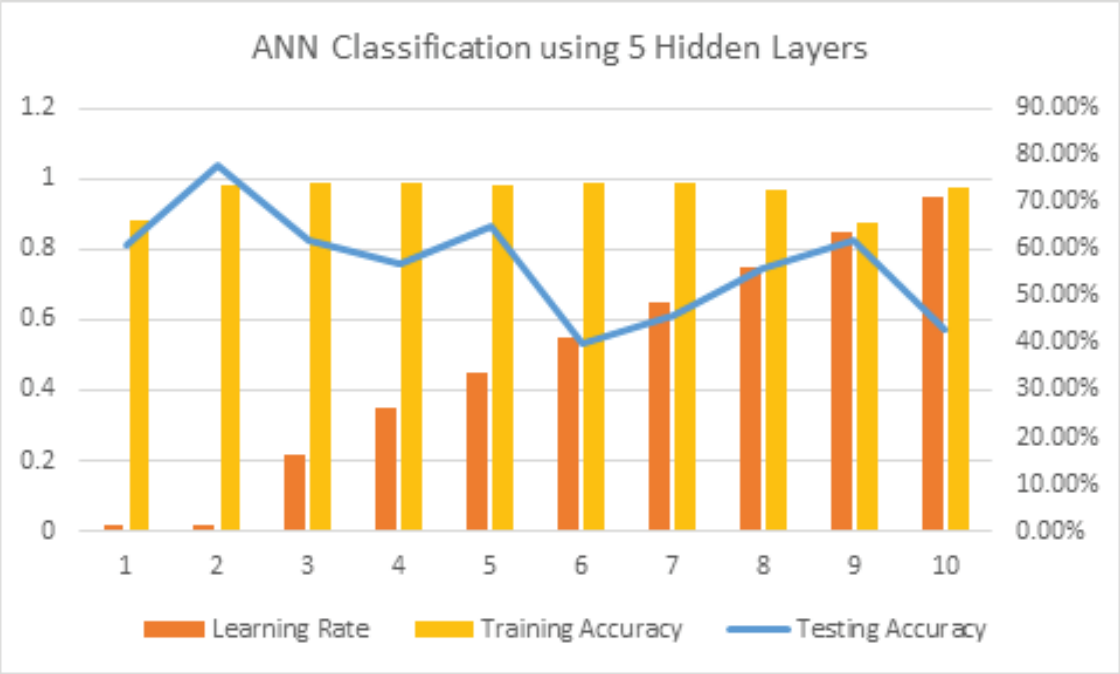

Fig.12 ANN Classification using 5 Hidden Layers

Fig. 12 shows the learning rate, training accuracy and testing accuracy on USGS data set using 5 hidden layers. By using ANN classifier achieved maximum 98% training accuracy and 78% testing accuracy.

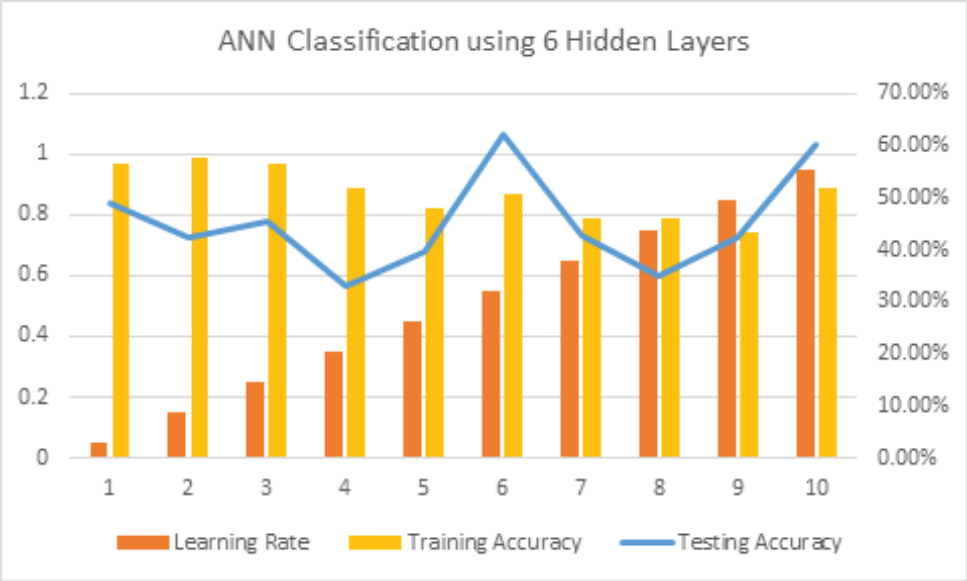

Fig. 13 ANN Classification using 6 Hidden Layers

Fig. 13 shows the learning rate, training accuracy and testing accuracy on USGS data set using 6 hidden layers. By using ANN classifier achieved maximum 98.69% training accuracy and 62.25% testing accuracy.

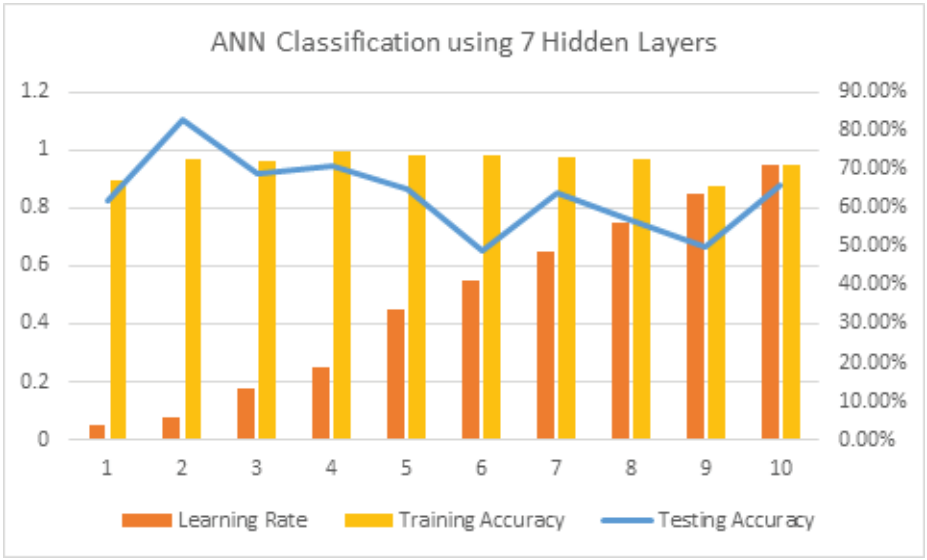

Fig.14 ANN Classification using 7 Hidden Layers

Fig. 14 shows the learning rate, training accuracy and testing accuracy on USGS data set using 7 hidden layers. By using ANN classifier achieved maximum 99.23% training accuracy and 62.25% testing accuracy.

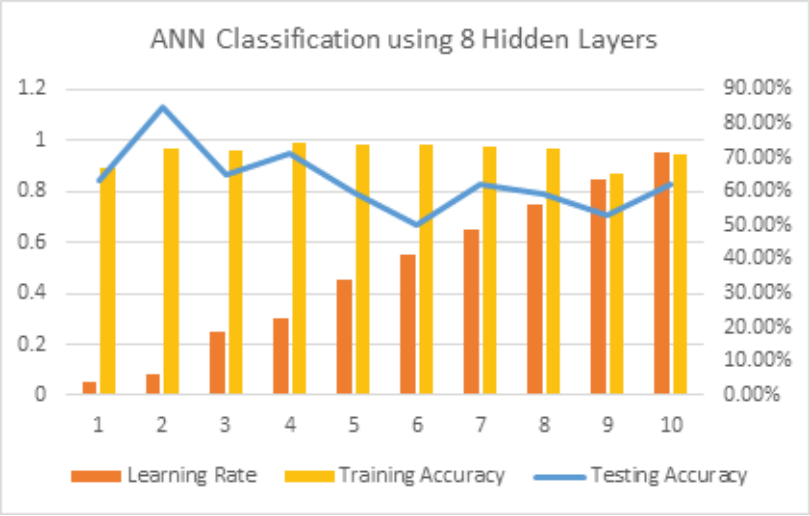

Fig.15 ANN Classification using 8 Hidden Layers

Fig. 15 shows the learning rate, training accuracy and testing accuracy on USGS data set using 8 hidden layers. By using ANN classifier achieved maximum 99.23% training accuracy and 85.00% testing accuracy.

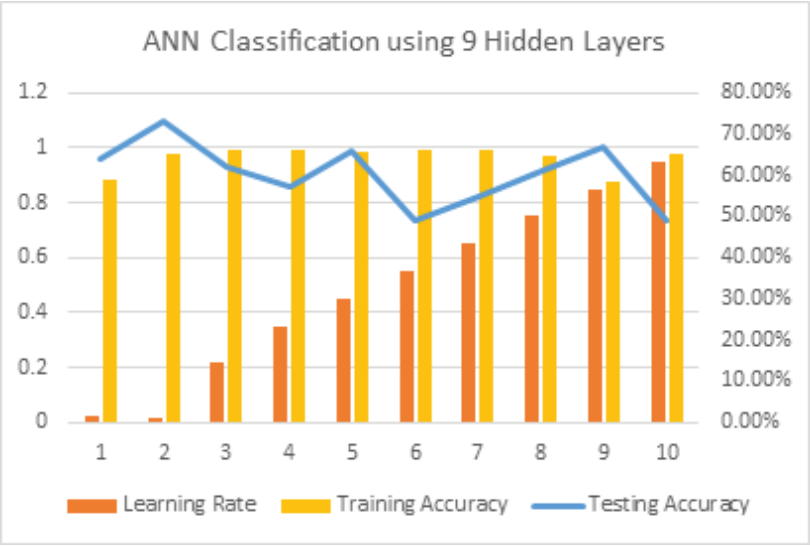

Fig.16 ANN Classification using 9 Hidden Layers

Fig. 16 shows the learning rate, training accuracy and testing accuracy on USGS data set using 9 hidden layers. By using ANN classifier achieved maximum 99.00% training accuracy and 73.00% testing accuracy.

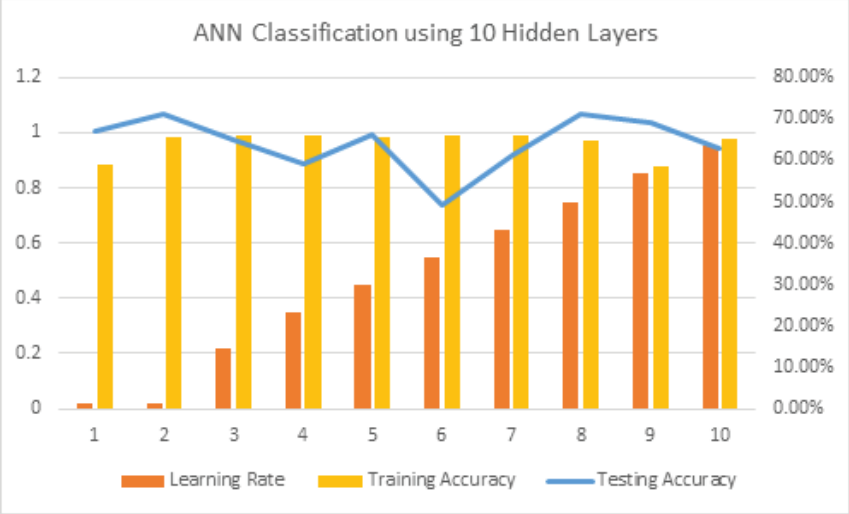

Fig.17ANN Classification using 10 Hidden Layers

Fig.17 shows the learning rate, training accuracy and testing accuracy on USGS data set using 10 hidden layers. By using ANN classifier achieved maximum 99.00% training accuracy and 71.00% testing accuracy.

4.1 Discussion

This work presented an effective approach for mapping rice in complicated landscapes. To extract the spectral/spatial and temporal properties of rice fields, deep learning and phenological metrics were coupled. Combining deep learning with phenological metrics may significantly increase remote sensing picture classification accuracy, particularly in rice mapping and crop land identification.

Crop area mapping utilizing remote sensing photography is critical for agricultural output. Rice, on the other hand, is often mapped by extracting time-series characteristics from Landsat data. Landsat8 spatial resolution is only appropriate for assessing big rice-growing regions and is insufficient for studying rice-growing areas in complicated landscapes. The current investigation was done using mid-range spatial resolution data, which caught the finer details that low-resolution data lost, but at a cheaper image-acquisition cost and over a greater area. The mid-spatial resolution categorization had no negative impact on accuracy (which topped 93.56%).

Our technique produced an accurate paddy rice map, although it has significant drawbacks. First, the

ANN structure chosen is determined by the research area's circumstances and the resolution of the remote sensing data. By modifying the activation function and parameter parameters, the current ANN model is optimized. The approach is appropriate for rice mapping in complicated landscape regions with fragmented rice distributions.

As a result, the ANN structure and optimum parameters must be adjusted to the circumstance. Second, the precision of phenological measurements is affected by the weather. Traditional agriculture desynchronizes crop phenological phases, and empirical knowledge-based judgment is intrinsically ambiguous. Third, due to the picture size difference between the pre-trained dataset and the fine-tuned dataset, the pre-trained data is compressed from 256 by 256 to 28 by 28, resulting in some information loss. Due to training data size constraints, we focused on the benefits of ANN in mining picture topology and texture characteristics, whereas the loss of color information in compression was disregarded.

Finally, the classification procedure is incapable of extracting and utilizing the deep properties of time-series data pictures. To dig further, the approach must concurrently understand the features of time-series characteristics and spectral/spatial characteristics.

The spectral, spatial, and temporal feature extractions should be combined into a single model in future study.

4.2 Temporal Analysis and Seasonal Variations in Cropland Dynamics.

The current study does acknowledge seasonal variations, but a more detailed temporal analysis could provide further insights into cropland dynamics, particularly in understanding the phenological stages of different crops. Such an analysis would involve examining changes over multiple growing seasons and correlating these changes with climatic and agricultural practices. This approach could help in predicting future trends and identifying the optimal times for satellite data acquisition. The decision not to pursue a detailed seasonal analysis in this study was primarily due to constraints related to data availability and processing capacity. Conducting a high-resolution temporal analysis would require access to more frequent satellite imagery, which may not always be available for all regions or time periods of interest. Additionally, the increased data volume and complexity would necessitate more advanced processing techniques and greater computational resources, which were beyond the scope of this study.

5 Conclusion

Due to the vast amount of accessible remote sensing satellite photos in recent decades, there has been

a tremendous demand to build machine learning classifiers. Classifiers take the role of the laborious and time-consuming digitizing procedure. Furthermore, there is a strong need to improve the performance accuracy of classifiers. The goal of this paper is to use neural networks as a machine-learning approach for LULC mapping. The Landsat 8 picture was captured using USGS and processed in Google Cloab&QGis for this study. The Sheikh Pura region of Pakistan was chosen as the research location for the analysis. The classifier was created using the TensorFlow ML framework in Python. In the classifier development step, a feedforward neural network structure is used. The training dataset was created using around 18050 sample points. The constructed classifier achieved an overall accuracy of 96% based on numerous trials. In general, the total accuracy grows in lockstep with the number of neurons in the first hidden layer. The findings demonstrate the ANN classifier's capability across several LULC classes. To summarize, the results demonstrate that using the ANN classifier effectively performed LULC mapping from Landsat 8 satellite photos in a reasonable amount of time with good performance accuracy. The ANN classifier may be used to categorize multispectral satellite pictures in regional and environmental studies. To create ANN classifiers for LULC mapping, the strong TensorFlow platform as an ML library is highly suggested. ANN classifiers can generate LULC maps quickly and with good results.

6 Future Work

Although the primary focus of this study was on satellite imagery and machine learning models for LULC classification, it is essential to recognize that climatic factors can have substantial effects on crop growth and land use patterns. To address this, the study incorporated meteorological data, such as temperature and precipitation records, from local weather stations to provide contextual information. However, the detailed analysis of extreme weather events and their direct impact on agricultural land use was not the primary focus. Future research will incorporate a more detailed climatic analysis. This could involve:

- **Long-Term Climate Data:** Analyzing long-term climatic trends and their correlation with agricultural practices. This approach would help in understanding how changes in climate patterns impact crop yields and land use over extended periods.
- **Extreme Weather Analysis:** Investigating the effects of specific extreme weather events, such as droughts, floods, and heat waves, on crop dynamics and land use changes. This analysis could be facilitated by integrating high-resolution weather data and historical event records with LULC data.
- **Model Integration:** Combining remote sensing data with climate models and

simulations to assess the potential impacts of future climate scenarios on agricultural systems. This integrated approach could provide a more comprehensive understanding of the interplay between climate factors and land use.

Future works will expand the scope by employing more effective technology such as other algorithms than those that are used, take advantage of cloud computing as well as further optimize the existing models. These endeavors will be geared towards achieving quick processing and low resource consumption without compromising the quality of results obtained from the predictive models.

References

1. W. Liu, J. Dong, K. Xiang, S. Wang, W. Han, and W. Yuan, "A sub-pixel method for estimating planting fraction of paddy rice in Northeast China," Remote Sens. Environ., vol. 205, pp. 305–314, 2018.

2. M. Boschetti et al., "PhenoRice: A method for automatic extraction of spatio-temporal information on rice crops using satellite data time series," Remote Sens. Environ., vol. 194, pp. 347–365, 2017.

3. E. Elert, "Rice by the numbers: A good grain.," Nature, vol. 514, no. 7524, pp. S50–S50, 2014.

4. S. Moharana and S. Dutta, "Spatial variability of chlorophyll and nitrogen content of rice from hyperspectral imagery," ISPRS J. Photogramm. Remote Sens., vol. 122, pp. 17–29, 2016.

5. Y. Shao et al., "Rice monitoring and production estimation using multitemporal RADARSAT," Remote Sens. Environ., vol. 76, no. 3, pp. 310–325, 2001.

6. M. Dabboor, B. Montpetit, and S. Howell, "Assessment of the high resolution SAR mode of the RADARSAT constellation mission for first year ice and multiyear ice characterization," Remote Sens., vol. 10, no. 4, p. 594, 2018.

7. Hasituya, Z. Chen, F. Li, and Hongmei, "Mapping plastic-mulched farmland with C-band full polarization SAR remote sensing data," Remote Sens., vol. 9, no. 12, p. 1264, 2017.

8. G. Cheng, P. Zhou, and J. Han, "Learning rotation-invariant convolutional neural networks for object detection in VHR optical remote sensing images," IEEE Trans. Geosci. Remote Sens., vol. 54, no. 12, pp. 7405–7415, 2016.

9. D. Marmanis, M. Datcu, T. Esch, and U. Stilla, "Deep learning earth observation classification using ImageNet pretrained networks," IEEE Geosci. Remote Sens. Lett., vol. 13, no. 1, pp. 105–109, 2015.

10. G. Fu, C. Liu, R. Zhou, T. Sun, and Q. Zhang, "Classification for high resolution remote sensing imagery using a fully convolutional network," Remote Sens., vol. 9, no. 5, p. 498, 2017.

11. X. Pan and J. Zhao, "A central-point-enhanced convolutional neural network for high-resolution remote-sensing image classification," Int. J. Remote Sens., vol. 38, no. 23, pp. 6554–6581, Dec. 2017, doi: 10.1080/01431161.2017.1362131.

12. C. Zhang et al., "A hybrid MLP-CNN classifier for very fine resolution remotely sensed image classification," ISPRS J. Photogramm. Remote Sens., vol. 140, pp. 133–144, 2018.

13. F. Hu, G.-S. Xia, J. Hu, and L. Zhang, "Transferring deep convolutional neural networks for the scene classification of high-resolution remote sensing imagery," Remote Sens., vol. 7, no. 11, pp. 14680–14707, 2015.

14. K. Nogueira, O. A. Penatti, and J. A. Dos Santos, "Towards better exploiting convolutional neural networks for remote sensing scene classification," Pattern Recognit., vol. 61, pp. 539–556, 2017.

15. C. Gómez, J. C. White, and M. A. Wulder, "Optical remotely sensed time series data for land cover classification: A review," ISPRS J. Photogramm. Remote Sens., vol. 116, pp. 55–72, 2016.

16. E. F. Lambin, M. D. Rounsevell, and H. J. Geist, "Are agricultural land-use models able to predict changes in land-use intensity?," Agric. Ecosyst. Environ., vol. 82, no. 1–3, pp. 321–331, 2000.

17. M. J. Steinhausen, P. D. Wagner, B. Narasimhan, and B. Waske, "Combining Sentinel-1 and Sentinel-2 data for improved land use and land cover mapping of monsoon regions," Int. J. Appl. Earth Obs. Geoinformation, vol. 73, pp. 595–604, 2018.

18. I. Becker-Reshef et al., "Strengthening agricultural decisions in countries at risk of food insecurity: The GEOGLAM Crop Monitor for Early Warning," Remote Sens. Environ., vol. 237, p. 111553, 2020.

19. Y. Xu et al., "Tracking annual cropland changes from 1984 to 2016 using time-series Landsat images with a change-detection and post-classification approach: Experiments from three sites in Africa," Remote Sens. Environ., vol. 218, pp. 13–31, 2018.

20. F. Q. Feng QuanLong, G. J. Gong JianHua, L. J. Liu JianTao, and L. Y. Li Yi, "Monitoring cropland dynamics of the Yellow River Delta based on multi-temporal Landsat imagery over 1986 to 2015.," 2015, Accessed: Feb. 25, 2024. [Online]. Available: https://www.cabidigitallibrary.org/doi/full/10.5555/20163010570

21. A. K. Whitcraft, I. Becker-Reshef, C. O. Justice, L. Gifford, A. Kavvada, and I. Jarvis, "No pixel left behind: Toward integrating Earth Observations for agriculture into the United Nations

Sustainable Development Goals framework," Remote Sens. Environ., vol. 235, p. 111470, 2019.

22. V. Maus, G. Câmara, M. Appel, and E. Pebesma, "dtwsat: Time-weighted dynamic time warping for satellite image time series analysis in r," J. Stat. Softw., vol. 88, pp. 1–31, 2019.

23. F. Petitjean, C. Kurtz, N. Passat, and P. Gançarski, "Spatio-temporal reasoning for the classification of satellite image time series," Pattern Recognit. Lett., vol. 33, no. 13, pp. 1805–1815, 2012.

24. R. Khatami, G. Mountrakis, and S. V. Stehman, "A meta-analysis of remote sensing research on supervised pixel-based land-cover image classification processes: General guidelines for practitioners and future research," Remote Sens. Environ., vol. 177, pp. 89–100, 2016.

25. D. K. Bolton, J. M. Gray, E. K. Melaas, M. Moon, L. Eklundh, and M. A. Friedl, "Continental-scale land surface phenology from harmonized Landsat 8 and Sentinel-2 imagery," Remote Sens. Environ., vol. 240, p. 111685, 2020.

26. M. Claverie et al., "The Harmonized Landsat and Sentinel-2 surface reflectance data set," Remote Sens. Environ., vol. 219, pp. 145–161, 2018.

27. A. Wolanin et al., "Estimating crop primary productivity with Sentinel-2 and Landsat 8 using machine learning methods trained with radiative transfer simulations," Remote Sens. Environ., vol. 225, pp. 441–457, 2019.

28. J. Inglada, A. Vincent, M. Arias, and C. Marais-Sicre, "Improved early crop type identification by joint use of high temporal resolution SAR and optical image time series," Remote Sens., vol. 8, no. 5, p. 362, 2016.

29. C. E. Woodcock, T. R. Loveland, and M. Herold, "Preface: Time series analysis imagery special issue," Remote Sens. Environ., vol. 238, p. 111613, 2020.

30. M. L. Ma Lei, L. M. Li ManChun, M. X. Ma XiaoXue, C. L. Cheng Liang, D. P. Du PeiJun, and L. Y. Liu YongXue, "A review of supervised object-based land-cover image classification.," 2017, Accessed: Feb. 25, 2024. [Online]. Available: https://www.cabidigitallibrary.org/doi/full/10.5555/20173278932

31. L. Zeng, B. D. Wardlow, D. Xiang, S. Hu, and D. Li, "A review of vegetation phenological metrics extraction using time-series, multispectral satellite data," Remote Sens. Environ., vol. 237, p. 111511, 2020.

32. M. Boschetti et al., "PhenoRice: A method for automatic extraction of spatio-temporal information on rice crops using satellite data time series," Remote Sens. Environ., vol. 194, pp. 347–365, 2017.

33. W. Liu, J. Dong, K. Xiang, S. Wang, W. Han, and W. Yuan, "A sub-pixel method for

estimating planting fraction of paddy rice in Northeast China," Remote Sens. Environ., vol. 205, pp. 305–314, 2018.

34. K. Nogueira, O. A. Penatti, and J. A. Dos Santos, "Towards better exploiting convolutional neural networks for remote sensing scene classification," Pattern Recognit., vol. 61, pp. 539–556, 2017.

35. L. Ghayour et al., "Performance evaluation of sentinel-2 and landsat 8 OLI data for land cover/use classification using a comparison between machine learning algorithms," Remote Sens., vol. 13, no. 7, p. 1349, 2021.

36. M. ED Chaves, M. CA Picoli, and I. D. Sanches, "Recent applications of Landsat 8/OLI and Sentinel-2/MSI for land use and land cover mapping: A systematic review," Remote Sens., vol. 12, no. 18, p. 3062, 2020.

37. A.-A. Kafy et al., "Assessment and prediction of seasonal land surface temperature change using multi-temporal Landsat images and their impacts on agricultural yields in Rajshahi, Bangladesh," Environ. Chall., vol. 4, p. 100147, 2021.

38. M. J. Ottman, B. A. Kimball, J. W. White, and G. W. Wall, "Wheat Growth Response to Increased Temperature from Varied Planting Dates and Supplemental Infrared Heating," Agron. J., vol. 104, no. 1, pp. 7–16, Jan. 2012, doi: 10.2134/agronj2011.0212.

39. G. C. Nelson et al., Food security, farming, and climate change to 2050: scenarios, results, policy options, vol. 172. Intl Food Policy Res Inst, 2010. Accessed: Feb. 25, 2024.

40. Z. C. Zhao Chuang et al., "Plausible rice yield losses under future climate warming.," 2017, Accessed: Feb. 25, 2024. [Online]. Available: https://www.cabidigitallibrary.org/doi/full/10.5555/20173068584

41. C. Losiri, M. Nagai, S. Ninsawat, and R. P. Shrestha, "Modeling urban expansion in Bangkok metropolitan region using demographic–economic data through cellular automata-Markov chain and multi-layer perceptron-Markov chain models," Sustainability, vol. 8, no. 7, p. 686, 2016.

42. F. Marini, J. Zupan, and A. L. Magrı, "On the use of counterpropagation artificial neural networks to characterize Italian rice varieties," Anal. Chim. Acta, vol. 510, no. 2, pp. 231–240, 2004.

43. F. Ramadhani, R. Pullanagari, G. Kereszturi, and J. Procter, "Mapping of rice growth phases and bare land using Landsat-8 OLI with machine learning," Int. J. Remote Sens., vol. 41, no. 21, pp. 8428–8452, Nov. 2020, doi: 10.1080/01431161.2020.1779378.

44. K. Clauss, M. Ottinger, and C. Kuenzer, "Mapping rice areas with Sentinel-1 time series and superpixel segmentation," Int. J. Remote Sens., vol. 39, no. 5, pp. 1399–1420, Mar. 2018, doi: 10.1080/01431161.2017.1404162.

45. Gumma, Nelson, and Yamano, "Mapping drought-induced changes in rice area in India," Int. J. Remote Sens., vol. 40, no. 21, pp. 8146–8173, Nov. 2019, doi: 10.1080/01431161.2018.1547456.

46. T. Sakamoto, M. Yokozawa, H. Toritani, M. Shibayama, N. Ishitsuka, and H. Ohno, "A crop phenology detection method using time-series MODIS data," Remote Sens. Environ., vol. 96, no. 3–4, pp. 366–374, 2005.

47. X. Xiao et al., "Mapping paddy rice agriculture in South and Southeast Asia using multi-temporal MODIS images," Remote Sens. Environ., vol. 100, no. 1, pp. 95–113, 2006.

48. C. Conrad, R. R. Colditz, S. Dech, D. Klein, and P. L. G. Vlek, "Temporal segmentation of MODIS time series for improving crop classification in Central Asian irrigation systems," Int. J. Remote Sens., vol. 32, no. 23, pp. 8763–8778, Dec. 2011, doi: 10.1080/01431161.2010.550647.

49. A. Veloso et al., "Understanding the temporal behavior of crops using Sentinel-1 and Sentinel-2-like data for agricultural applications," Remote Sens. Environ., vol. 199, pp. 415–426, 2017.

50 A. Veloso et al., "Understanding the temporal behavior of crops using Sentinel-1 and Sentinel-2-like data for agricultural applications," Remote Sens. Environ., vol. 199, pp. 415–426, 2017.

51. Y. Ban, P. Zhang, A. Nascetti, A. R. Bevington, and M. A. Wulder, "Near real-time wildfire progression monitoring with Sentinel-1 SAR time series and deep learning," Sci. Rep., vol. 10, no. 1, p. 1322, 2020.

52. M. Han, X. Zhu, and W. Yao, "Remote sensing image classification based on neural network ensemble algorithm," Neurocomputing, vol. 78, no. 1, pp. 133–138, 2012.

53. J. Ding, B. Chen, H. Liu, and M. Huang, "Convolutional neural network with data augmentation for SAR target recognition," IEEE Geosci. Remote Sens. Lett., vol. 13, no. 3, pp. 364–368, 2016.

54. Q. Feng, J. Gong, J. Liu, and Y. Li, "Monitoring cropland dynamics of the Yellow River Delta based on multi-temporal Landsat imagery over 1986 to 2015," Sustainability, vol. 7, no. 11, pp. 14834–14858, 2015.

55. J. Geng, J. Fan, H. Wang, X. Ma, B. Li, and F. Chen, "High-resolution SAR image classification via deep convolutional autoencoders," IEEE Geosci. Remote Sens. Lett., vol. 12, no. 11, pp. 2351–2355, 2015.